

Product Detection Study of the Gas-phase Oxidation of Methylphenyl Radicals using Synchrotron Photoionisation Mass Spectrometry

Matthew B. Prendergast,¹

Benjamin B. Kirk,¹

John D. Savee,² David L. Osborn,² Craig A. Taatjes,²

Patrick Hemberger³

Stephen J. Blanksby,⁴

Gabriel da Silva,⁵

Adam J. Trevitt^{1}*

Supporting Information

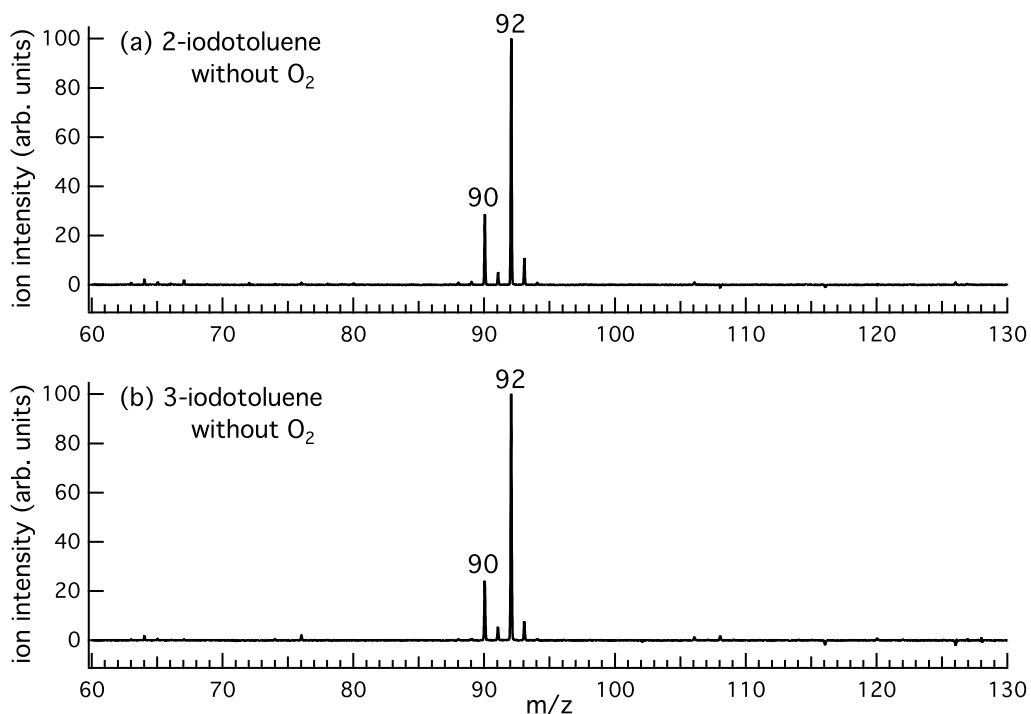


Figure S1. Photoionisation mass spectra at 10.2 eV integrated 0–80 ms after 248 nm photolysis of (a) *o*-iodotoluene and (b) *m*-iodotoluene without O₂ added to the reactor and at ambient temperatures (approximately 303 K).

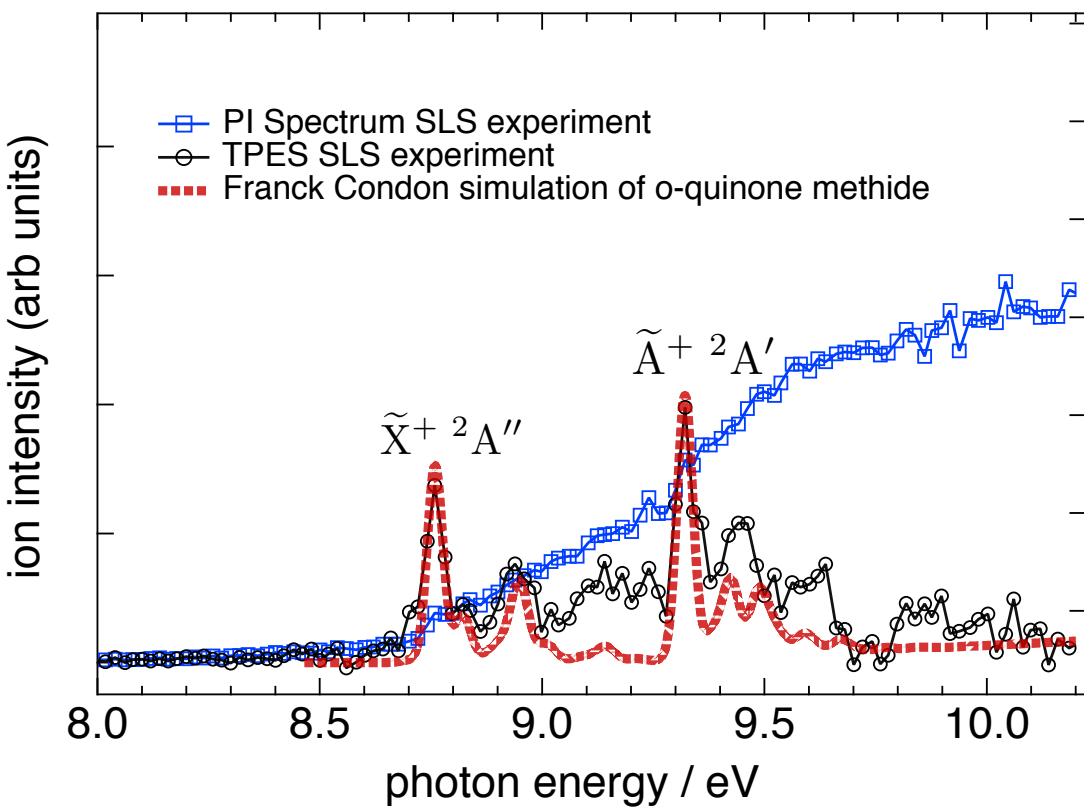


Figure S2. (blue squares) The m/z 106 photoionization product from the pyrolysis of *o*-methylanisole conducted at the SLS (black circles). The photoion mass-selected threshold photoelectron spectrum (ms-TPES) from the same experiment is compared to (red dash) simulations of the $X^+ \leftarrow X$ and $A^+ \leftarrow X$ Franck Condon transitions for *o*-quinone methide ($o\text{-CH}_2\text{C}_6\text{H}_4=\text{O}$, as described in the main text). The Franck Condon simulations use the geometries of the neutral and ion ground state, optimised at the B3LYP/6-311++G(d,p) level of theory (Gaussian 16, Revision A.03),¹ while the same level was also utilised for the excited ion state, however applying the time-dependent (TD) approach. The Franck Condon factors with the program ezSpectrum.² Stick spectra were convoluted with 40 meV FWHM Gaussian functions and shifted in energy to best align with the experimental spectrum.

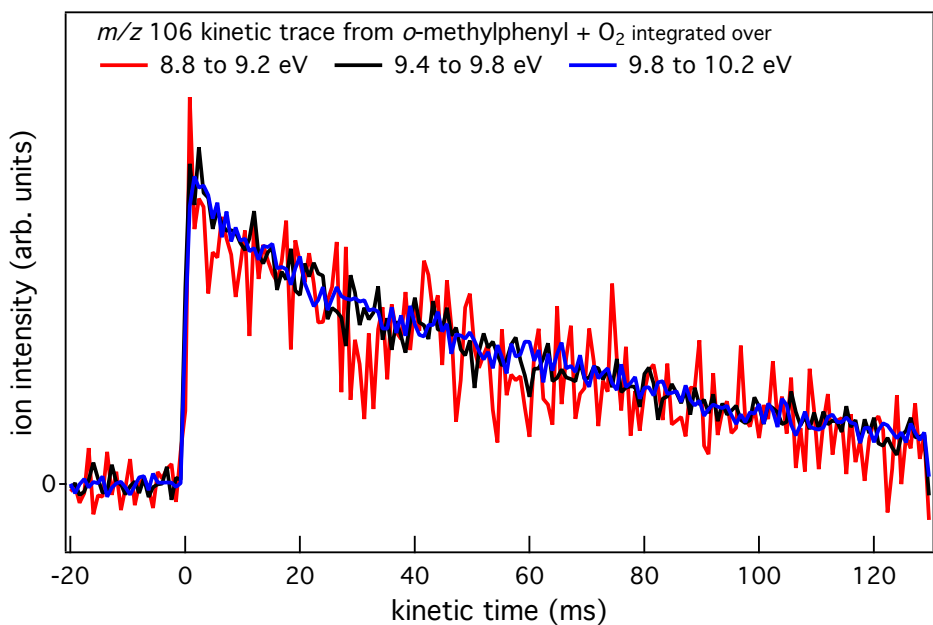


Figure S3. Kinetic traces of *m/z* 106 integrated between 8.8–9.2 eV (red), 9.4–9.8 eV (black) and 9.8–10.2 eV (blue) from *o*-methylphenyl + O₂ at ambient temperatures. The abscissa of the graph is time relative to the photolysis laser pulse. The *m/z* 106 ion signal is shown to be laser dependent and the kinetic traces have identical profiles within signal-to-noise over the three photoionisation energy ranges.

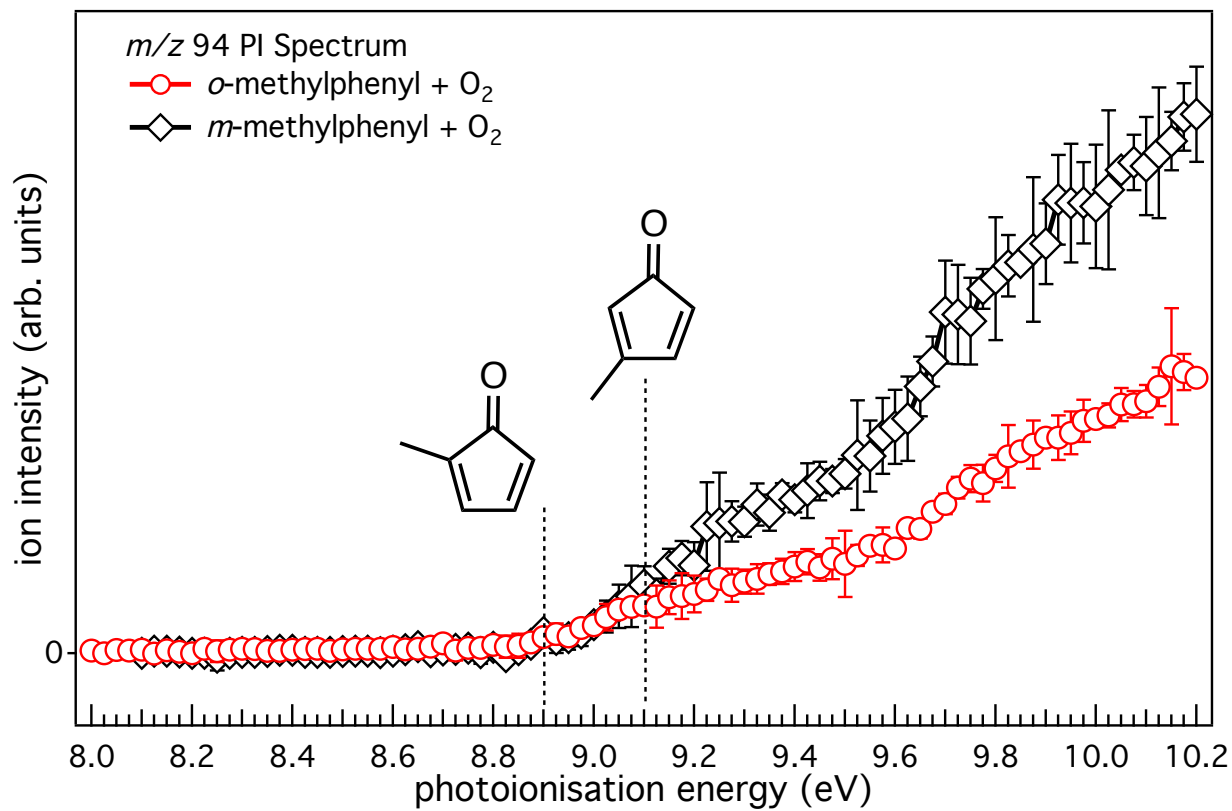


Figure S4. Photoionisation spectra integrated 0–80 ms after photolysis for *m/z* 94 from *o*-methylphenyl + O₂ (red open circles) and *m*-methylphenyl + O₂ (black open diamonds), representing an average of three PI spectra with error bars representing 2 standard deviations. The PI spectrum from *o*-methylphenyl + O₂ is assigned 2-methylcyclopentadieneone. The PI spectrum from *m*-methylphenyl + O₂ is assigned as a mixture of 2- and 3-methylcyclopentadieneone. The spectra are scaled to overlap between 8.9 and 9.1 eV for comparison.

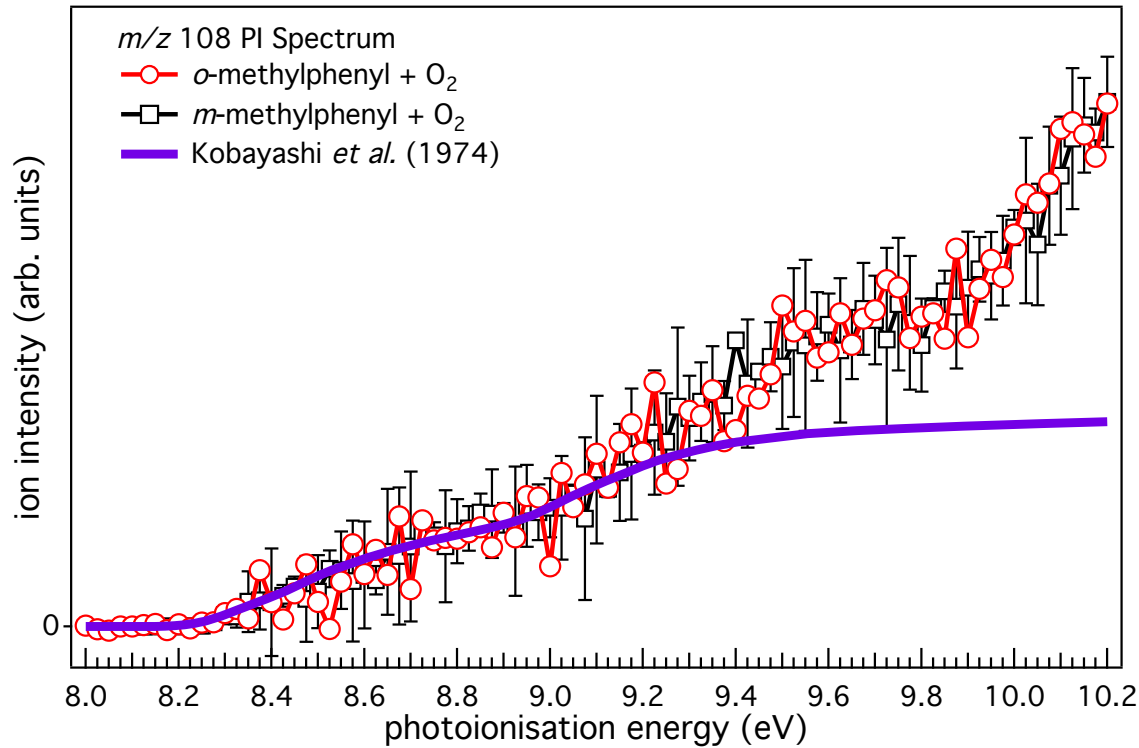


Figure S5. Photoionisation spectra integrated 0–80 ms after photolysis for *m*/z 108 from *m*-methylphenyl + O₂ (black open squares) and σ -methylphenyl + O₂ (open red circles). An integrated PE spectrum for *m*-cresol (Kobayashi *et al.*, Ref.³) and all traces are scaled to overlap between 8.2–9.2 eV. As the signal levels are low, the error bars are omitted for the σ -methylphenyl case. This product channel is not assigned as a primary reaction product as discussed in the main text.

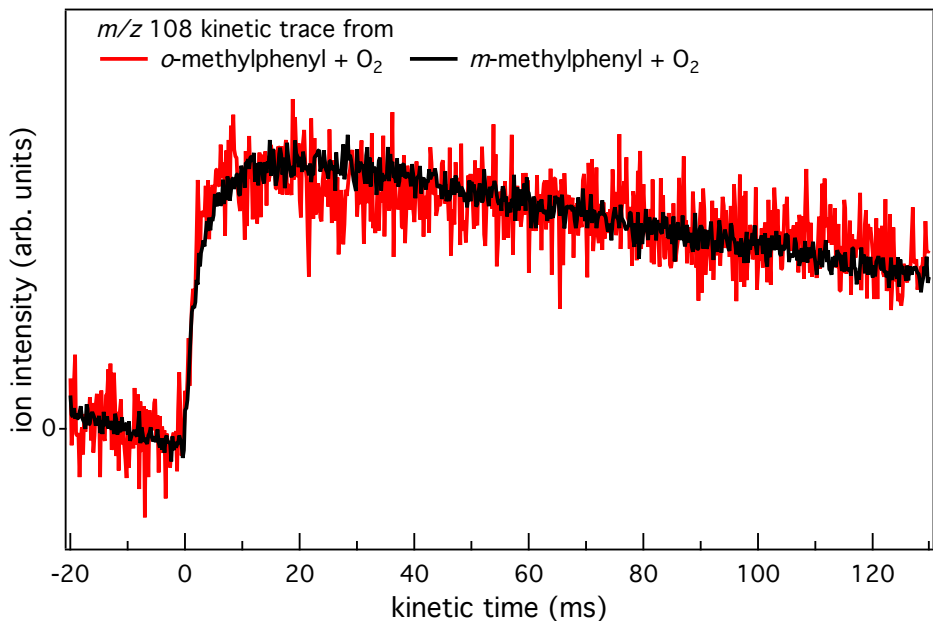


Figure S6. Co-added *m/z* 108 kinetic traces at 10.2 eV and ambient temperature. The traces, timed relative to the photolysis laser pulse, show laser dependent signal that increases intensity gradually until 20 ms after the laser pulse. The rate coefficient for *m/z* 108 appearance from *o*- and *m*-methylphenyl + O₂ is $500 \pm 70 \text{ s}^{-1}$ and $400 \pm 20 \text{ s}^{-1}$ respectively between 0–10 ms after photolysis, with the uncertainty representing 1 standard deviation.

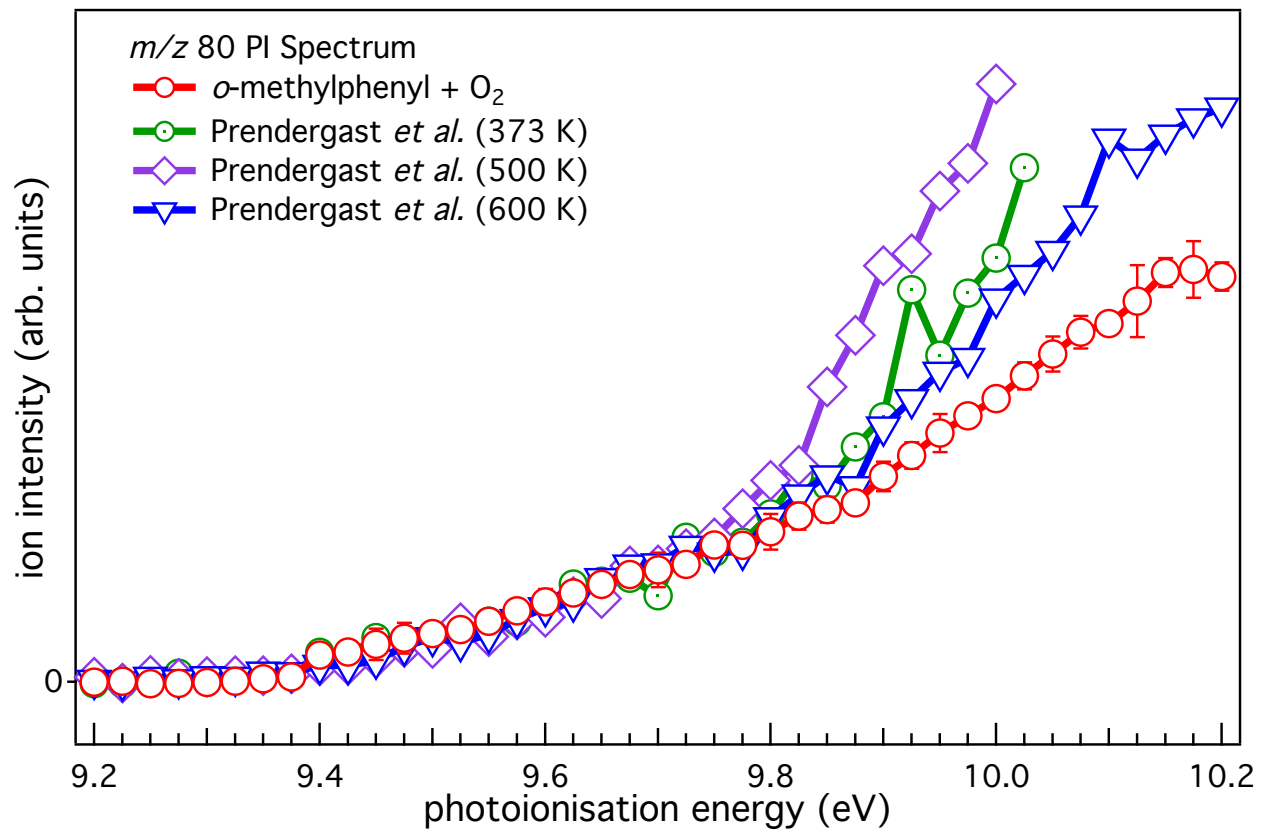


Figure S7. Photoionisation spectrum integrated 0–80 ms after photolysis for *m/z* 80 from *o*-methylphenyl + O₂ (red open circles) with error bars representing 2 standard deviations is compared to *m/z* 80 PI spectra for cyclopentadienone from *o*-hydroxyphenyl + O₂, which is affected by dissociative ionisation of *o*-benzoquinone at 9.8 eV.⁴ The absence of an enhanced signal between 9.8–10 eV indicates *o*-benzoquinone has insufficient quantities to affect the *m/z* 80 PI spectrum from *o*-methylphenyl + O₂.

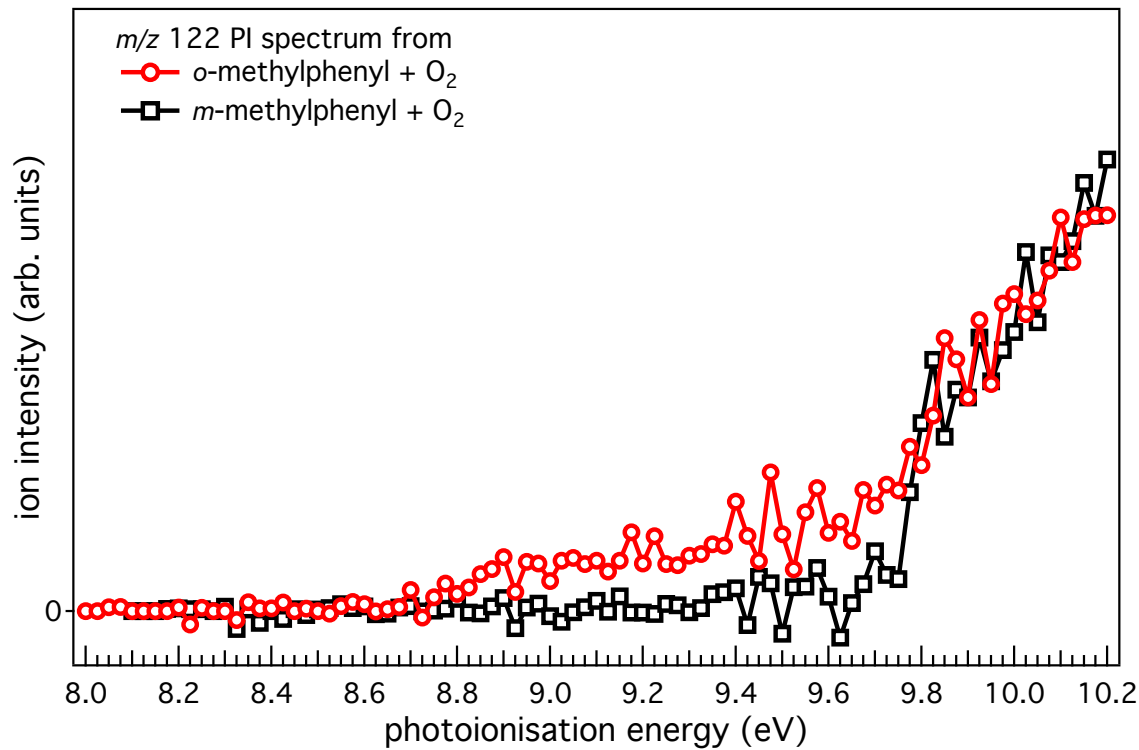


Figure S8 Photoionisation spectra integrated 0–80 ms after photolysis for *m/z* 122 from o-methylphenyl + O₂ (red open circles) and m-methylphenyl + O₂ (black open squares). As the signal levels are low, the error bars are omitted for clarity. This product channel is not assigned as a primary reaction product as discussed in the main text.

Table S1. Calculated CBS-QB3 adiabatic ionisation energies for C₇H₆O isomers (106 Da). The CBS-QB3 enthalpies (ΔH_f) are provided in kcal mol⁻¹ with zero-point energy.

C ₇ H ₆ O isomers	Calculated adiabatic IE (eV)	Literature IE (eV)	Relative ΔH_f (kcal mol ⁻¹)
cyclohexa-2,4-dien-1-ylidene methanone	7.4		36.0
(Z)-hepta-1,3,5,6-tetraenone	7.6		63.2
(Z)-hepta-1,3-dien-5-ynone	7.8		59.8
2-methyl-cyclopenta-2,4-dien-1- ylidenemethanone	7.9		26.6
hepta-1,5-dien-3-ynone	7.9		63.6
2-vinyl-cyclopentadienone	8.4		36.2
7-oxabicyclo[4.2.0]octa-1(6),2,4- triene	8.4		32.6
<i>o</i> -quinone methide	8.7	8.80 (vertical) ⁵	23.1
tropone (alias cyclohepta-2,4,6-trienone)	8.8	8.88 ± 0.05 (adiabatic) ⁶	25.0
(Z)-hepta-4,6-dien-2-ynal	8.9		66.5
hepta-4,6-diynal	8.9		80.4
(Z)-hepta-2,6-dien-4-ynal	9.0		65.0
(2Z,4Z)-hepta-2,4-dien-6-ynal	9.0		62.8
<i>p</i> -quinone methide	9.2		19.9
benzaldehyde	9.6	9.5 (adiabatic) ⁷⁻⁸	0.0
hepta-2,4-diynal	9.6		78.8

Table S2. Calculated CBS-QB3 adiabatic ionisation energies for C₇H₇O isomers (107 Da). The CBS-QB3 enthalpies (ΔH_f) are provided in kcal mol⁻¹ with zero-point energy.

C ₇ H ₇ O isomers	Calculated adiabatic IE (eV)	Literature IE (eV)	Relative ΔH_f (kcal mol ⁻¹)
4-methylphenoxy radical	8.3		1.0
2-methylphenoxy radical	8.4		0.0
3-methylphenoxy radical	8.5		1.8

Table S3. Calculated CBS-QB3 adiabatic ionisation energies for C₇H₆O₂ isomers (122 Da). The CBS-QB3 enthalpies (ΔH_f) are provided in kcal mol⁻¹ with zero-point energy.

C ₇ H ₆ O ₂ isomers	Calculated adiabatic IE (eV)	Literature IE (eV)	Relative ΔH _f (kcal mol ⁻¹)
4-hydroxy-1,2-quinone methide	8.2		28.4
6-hydroxy-1,2-quinone methide	8.2		31.3
3-hydroxy-1,2-quinone methide	8.3		28
3-methide-oxepinone	8.3		38.9
5-hydroxy-1,2-quinone methide	8.5		25.1
7-methide-oxepinone	8.5		38.5
2-hydroxy-1,4-quinone methide	8.7		19.9
2-hydroxy-benzaldehyde	8.7		0.0
4-hydroxy-benzaldehyde	8.8		5.1
3-hydroxy-benzaldehyde	8.9		5.3
4-methyl-1,2-benzoquinone	9		27.7
3-methyl-1,2-benzoquinone	9.1		27.5
3-hydroxy-1,4-quinone methide	9.1		23.4
2-methyl-1,4-benzoquinone	10		19.1

Table S4. TI diagnostic values CCSD(T)/6-31G(d) for stationary points around the bifurcation.

Structure	TA DIAG value
<i>o</i> ROO	0.021
<i>m</i> ROO	0.023
<i>o</i> TS1	0.078
<i>o</i> TS2	0.047
<i>m</i> TS1	0.040
<i>m</i> TS2	0.039

References

1. Frisch, M. J.; Trucks, G. W.; Schlegel, H. B.; Scuseria, G. E.; Robb, M. A.; Cheeseman, J. R.; Scalmani, G.; Barone, V.; Petersson, G. A.; Nakatsuji, H.; Li, X.; Caricato, M.; Marenich, A. V.; Bloino, J.; Janesko, B. G.; Gomperts, R.; Mennucci, B.; Hratchian, H. P.; Ortiz, J. V.; Izmaylov, A. F.; Sonnenberg, J. L.; Williams; Ding, F.; Lipparini, F.; Egidi, F.; Goings, J.; Peng, B.; Petrone, A.; Henderson, T.; Ranasinghe, D.; Zakrzewski, V. G.; Gao, J.; Rega, N.; Zheng, G.; Liang, W.; Hada, M.; Ehara, M.; Toyota, K.; Fukuda, R.; Hasegawa, J.; Ishida, M.; Nakajima, T.; Honda, Y.; Kitao, O.; Nakai, H.; Vreven, T.; Throssell, K.; Montgomery Jr., J. A.; Peralta, J. E.; Ogliaro, F.; Bearpark, M. J.; Heyd, J. J.; Brothers, E. N.; Kudin, K. N.; Staroverov, V. N.; Keith, T. A.; Kobayashi, R.; Normand, J.; Raghavachari, K.; Rendell, A. P.; Burant, J. C.; Iyengar, S. S.; Tomasi, J.; Cossi, M.; Millam, J. M.; Klene, M.; Adamo, C.; Cammi, R.; Ochterski, J. W.; Martin, R. L.; Morokuma, K.; Farkas, O.; Foresman, J. B.; Fox, D. J. *Gaussian 16 Rev. A.03*, Wallingford, CT, 2016.
2. Mozhayskiy, V. A.; Krylov, A. I., *ezSpectrum*, <http://iopenshell.usc.edu/downloads>.
3. Kobayashi, T.; Nagakura, S., *Bull. Chem. Soc. Jpn.* **1974**, *47* (10), 2563-2572.
4. Prendergast, M. B.; Kirk, B. B.; Savee, J. D.; Osborn, D. L.; Taatjes, C. A.; Masters, K.-S.; Blanksby, S. J.; da Silva, G.; Trevitt, A. J., *Phys. Chem. Chem. Phys.* **2016**, *18*, 4320-4332.
5. Eck, V.; Schweig, A.; Vermeer, H., *Tetrahedron Lett.* **1978**, *19* (27), 2433-2436.
6. Lias, S. G.; Bartmess, J. E.; Liebman, J. F.; Holmes, J. L.; Levin, R. D.; Mallard, W. G., Ion Energetics Data. In *NIST Chemistry WebBook*, *NIST Standard Reference Database Number 69*, Linstrom, P. J.; Mallard, W. G., Eds. National Institute of Standards and Technology: Gaithersburg MD, 20899, 2011.
7. Zhou, Z.; Xie, M.; Wang, Z.; Qi, F., *Rapid Commun. Mass Spectrom.* **2009**, *23* (24), 3994-4002.
8. Rosenstock, H. M.; Draxl, K.; Steiner, B. W.; Herron, J. T., Ion Energetics Data. In *NIST Chemistry WebBook*, *NIST Standard Reference Database Number 69*, Linstrom, P. J.; Mallard, W. G., Eds. National Institute of Standards and Technology: Gaithersburg MD, 20899, 2011.
9. Lias, S. G.; Levin, R. D.; Kafafi, S. A., Ion Energetics Data. In *NIST Chemistry WebBook*, *NIST Standard Reference Database Number 69*, Linstrom, P. J.; Mallard, W. G., Eds. National Institute of Standards and Technology: Gaithersburg MD, 20899, 2011.